THE GAMMA-RADIATION FROM THE BOMBARDMENT OF HEAVY ICE WITH LOW-ENERGY PROTONS

by

Colin David Scarfe

B.Sc. University of British Columbia 1960

A THESIS SUBMITTED IN PARTIAL FULFILLMENT OF THE REQUIREMENTS FOR THE DEGREE OF MASTER OF SCIENCE

in the department of

PHYSICS

We accept this thesis as conforming to the required standard

The University of British Columbia

October 1961

In presenting this thesis in partial fulfilment of the requirements for an advanced degree at the University of British Columbia, I agree that the Library shall make it freely available for reference and study. I further agree that permission for extensive copying of this thesis for scholarly purposes may be granted by the Head of my Department or by his representatives. It is understood that copying or publication of this thesis for financial gain shall not be allowed without my written permission.

Department of Physics

The University of British Columbia,
Vancouver 8, Canada.

Date September 7, 1961

ABSTRACT

The reaction $D(p, \gamma)He^3$ was studied at incident proton energies of less than 50 kev. The method was to bombard heavy ice targets with the proton beam from the 50 kv accelerator. This machine develops an intense beam of 60 to 80 microamps which is necessary to produce a substantial yield despite the low reaction cross section.

The angular distribution of the γ-rays was found to follow a $(\sin^2\theta + B)$ pattern as expected from earlier work carried out at higher energies. In the neighborhood of 35 kev the value of B was found, by measurements of the yield at 90° and at 0° to the incident beam direction, to be $.283 \pm .110$.

The total cross section was found to take on the following values:

E(kev)	$\sigma (cm^2) \times 10^{-32}$
29.1	4.87 ± 1.05
37.5	11.2 ± 2.8
44.0	12.9 ± 4.0

ACKNOWLEDGEMENTS

The author wishes to express his gratitude to Dr. G. M. Griffiths who suggested and supervised this work, and whose unfailing assistance and advice during the performance of the experiment and with the writing of this thesis are greatly appreciated.

Thanks also are due to Mr. M. Lal for his valuable advice in the initial stages and to Mrs. E. Nesbitt, who typed this thesis.

The author gratefully acknowledges the receipt of a National Research Council of Canada bursary.

TABLE OF CONTENTS

ILLUSTRATIONS

The purpose of this thesis is to discuss an experiment with the reaction $D(p,\gamma)He^3$. This reaction is of special interest in nuclear physics because it yields information about the three body system He^3. A study of three-body nuclei should lead to a more detailed understanding of internucleon forces than is possible from a study of the deuteron, the only bound two-nucleon system, because of the somewhat tighter binding of the three-body system and because of the possibility of finding many-body forces different from ordinary two-body forces.

Curran and Strothers (1939) were the first to report detection of the gamma radiation from this reaction. Later, Fowler, Lauritsen and Tollestrup (1949) found that the angular distribution from a thick ice target at a bombarding energy of 1.4 Mev had the form $A(\sin^2\theta + B)$ where B was small. They also found that the total cross section in the region 0.5 to 1.7 Mev obeyed the relation $\sigma = 0.74E^{0.72} \times 10^{-29}$ cm^2 where E is in Mev.

Further study by Wilkinson (1952) showed that the main contribution to the radiation is electric dipole in character. Griffiths and Warren (1955) checked the measurement of the absolute cross-section made by Fowler et.al. and made a detailed study of the angular distribution with the following results.

E_p(Mev)	B
1.75	0.025±0.006
1.0	0.046±0.005
0.8	0.04±0.015
0.6	0.026±0.010

With a considerable improvement in target thickness measurements and an accurate measurement of the scintillation counter efficiency, the angular distribution and absolute cross-section have been remeasured by Larson (1957) and by Griffiths, Larson and Robertson (to be published) with the following results:

E_p(Mev)	B	$\sigma \times 10^{-30}$
1.0	0.024±0.003	3.24±0.35
0.6	0.032±0.004	--------
0.3	0.079±0.010	0.898±0.097

This increase in B with decreasing energy suggests that the contribution at 0^o is due to an s-wave process rather than to the p-wave capture leading to the $\sin^2\theta$ distribution. A more detailed study of this is of considerable interest in the theory of nuclear forces.

Because of this and because the reaction is significant in astrophysical processes at very low energies it was felt that an experimental measurement at an energy well below 300kev would be of value, particularly because at the present time, it is impossible to predict the cross-section reliably at very low energies by extrapolating from the higher energy results. There are three reasons for this.

Firstly, the process occurs by a direct reaction mechanism which is rather sensitive to external portions of the nuclear wave function which are not very well understood. Secondly, the low Coulomb barrier means that the energy dependence of the reaction is influenced by factors other than the usual exponential penetrability which is often assumed for low energy reactions. Thirdly, the energy dependence of the angular distribution shown above suggests that two processes contribute to the capture with different energy dependences. At the higher energies the p-wave capture with electric dipole emission clearly predominates. However, if the small isotropic component is due to an s-wave process, which seems likely to be the case on the basis of the angular distribution data of Larson (1957) then this process is likely to predominate at very low energies.

The first measurements in the 25 to 45 kev region were made by Lal (1961) who showed clearly that the γ-rays could be observed at these energies and who made a preliminary measurement of the angular distribution.

The $D(p,\gamma)He^3$ measurements at the higher energies were hampered by the presence of neutrons produced by the reaction $D(d,n)He^3$ between recoil deuterons and deuterons in the target. A detailed study of this effect has been made by Singh et al.(1959). The neutron yield, quite appreciable at 1 Mev bombarding energy, decreases very rapidly with energy and is expected to be negligible at

energies below 50 kev, which were used in the present work.

The previously mentioned astrophysical importance of the reaction $D(p,\gamma)He^3$ is twofold. Firstly, it is a link in the proton-proton chain, which is the principal source of energy in the lower-temperature main-sequence stars such as our sun. In addition the cross-section at very low energies may be of importance because, as Cameron (1960) pointed out, it is one of the first reactions to occur as a star is condensing from the galactic gas onto the main sequence. The resulting radiation pressure prevents further contraction until the deuterium initially present is consumed. Thus the amount of deuterium present in interstellar space affects the time-scale for stellar condensation through the reaction $D(p,\gamma)He^3$. The present work was undertaken in an attempt to answer some of these questions.

CHAPTER II - APPARATUS

1. The 50 kv set

The proton beam required for this experiment was obtained from the 50 kv accelerator described by Kirkaldy (1951). Hydrogen from a steel storage bottle was admitted to a pyrex discharge tube by means of an electrically heated thermal leak. The discharge tube was surrounded by the tank coil of a 25 mc 300-watt oscillator, which ionised the gas. The protons were drawn from the discharge tube through a small (.06") hole by means of a bottom extraction probe potential. They were then accelerated down a column by means of a continuously variable d.c. potential produced by a Ferranti 50-kv X-Ray transformer rectifier set with a separate smoothing filter. The voltage was determined by measuring the current through a 60 megohm resistor chain. The beam was focussed by two electrostatic lenses in the accelerating column, the first just below the extractor and the second several inches lower. Since the second lens operated on the main accelerating potential, the focus was markedly dependent on the operating voltage, being much better at high energies than at low.

Due to incomplete ionisation and recombination in the ion source the beam consisted partly of H_2^+ and H_3^+ (the latter greatly enhanced by the presence of traces of nitrogen). Normal percentages of molecular ions were as follows:

	Normal Operation	With small air leak
H^+	75%	50%
H_2^+	15%	20%
H_3^+	10%	30%

Due to their different charge-to-mass ratio , however, these components were easily separated by a water-cooled electromagnet located at the lower end of the accelerating column. This also served to bend the H^+ beam through 90° so that it was travelling horizontally.

A 1.2 cm by 0.6 cm definint slit was located $8\frac{1}{2}$" beyond the magnet exit, attached to the bottom of a liquid air trap which served to prevent condensable vapors from contaminating the target. The defining slit was maintained at +90 volts in order to inhibit the emission of secondary electrons and also to collect the secondary electrons emitted by the other metal surfaces in the tube. A wire gauze prevented charge from collecting on the areas of glass surface in the tube.

The heavy water target was frozen on a copper backing plate attached to the bottom of another liquid air trap and located $7\frac{1}{2}$" beyond the defining slit. The backing plate and trap could be raised to lay a target or lowered into the beam, as shown in figure 1. The target was held at +150V to suppress secondary electron emission.

The D_2O dispenser consisted of a small vial of D_2O together with an oil manometer. A volume of D_2O vapor at a pressure indicated by the manometer was allowed to

FIG. 1

TARGET CHAMBER

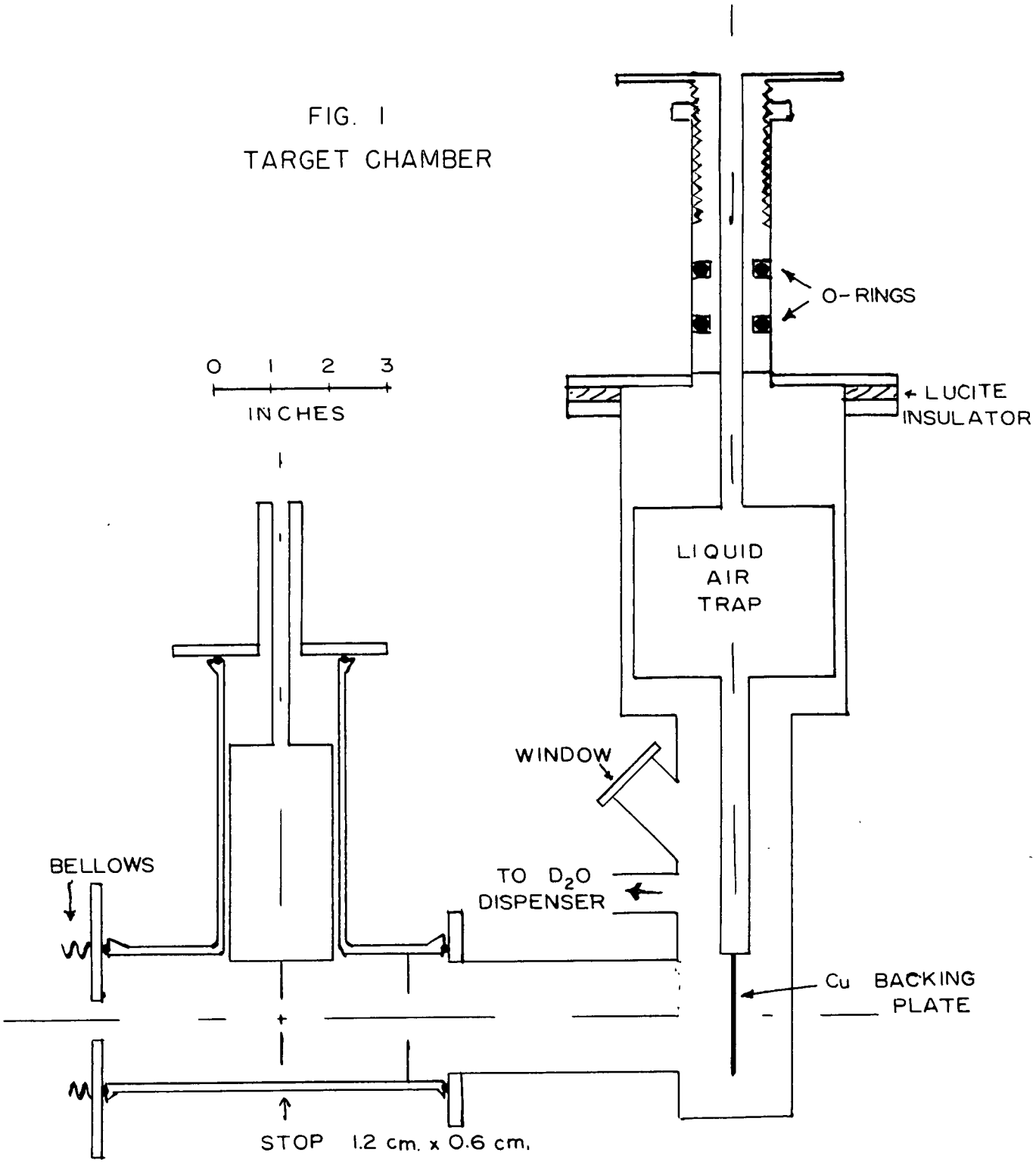

diffuse through a glass wool plug and to freeze in a thin layer on the backing plate. Since the only requirement for this experiment was that the target be thick enough to stop the beam entirely, no detailed measurement of target thickness was required.

A pressure of 10^{-5}mm Hg was required to prevent excessive attenuation of the beam by collision with air molecules. This was maintained by means of a Distillation Products 275 liter/sec. oil diffusion pump together with a Cenco Megavac rotary pump. Condensable vapors were frozen out on a large liquid air trap above the diffusion pump. An auxiliary valve system at the exit end of the magnet allowed the target chamber and defining slit to be removed without letting air into the source and accelerating column. The system pressure was measured by means of a Pirani gauge and a Sylvania VG1 ionisation gauge.

The beam current available varied considerably with the accelerating potential. Above 35kv., a current of 60 to 80 microamp could be obtained at the target. At 24kv., however, the best obtainable target current was about 25 microamp.

2. Counter and Electronics

The $D(p,\gamma)He^3$ γ-rays were detected by a Harshaw thallium activated sodium iodide scintillation counter. The crystal was cylindrical, 4.50 ± 0.005 inches long and 2.75 ± 0.005 inches in diameter. Its front surface was located 0.407 ± 0.030 inch from the front of its aluminum container.

The crystal was optically coupled to a Dumont K1213 photomultiplier tube, whose output was fed into a preamplifier. The preamplifier circuit and the wiring diagram of the photomultiplier are shown in figures 2 and 3. The crystal, photomultiplier and preamplifier were all housed in a 16" length of 4" diameter brass tube. The output from preamplifier was further amplified and fed into the laboratory's Computing Devices of Canada one hundred-channel Kicksorter for spectrum analysis.

The counter efficiency had previously been measured using the $F^{19}(p,\alpha\gamma)O^{16}$ reaction. The efficiency is defined as the ratio of the number of counts above the half-energy bias to the number of gamma rays incident on an area equal to that of the crystal face and located at the effective center of the crystal. The depth of the effective center is defined as the distance which must be added to the source-to-crystal face distance to give an inverse-square law relation between number of counts and distance. For 6.14 Mev γ-rays the effective center is 5.5 ± 0.5 cm behind the front of the aluminum can and its efficiency is .761. This corresponds to an effective center depth of 5.4 ± 0.5 cm and an efficiency of .73 for the 5.5 Mev γ-rays detected in this experiment.

The gain of the system and the kicksorter bias varied with time and so it was necessary to calibrate the system before and after each run. This was done by measuring the spectrum of a radiothorium (Th^{228}) source. The final step in this decay chain is the emission of a 2.615 Mev

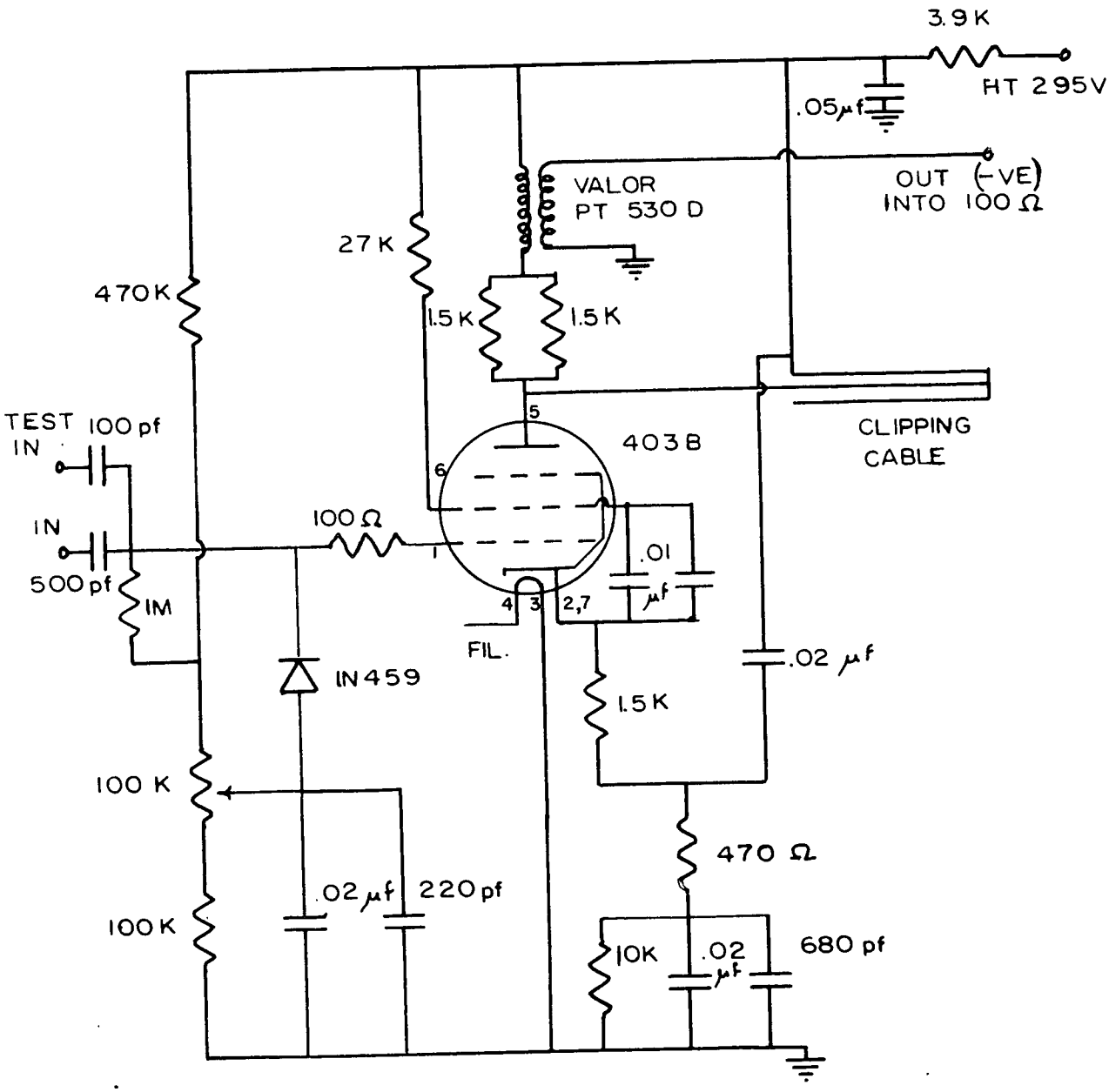

FIG: 2 HEAD AMPLIFIER

gamma ray. The linearity of the system was checked by turning off the high tension on the photomultiplier and connecting a mercury relay pulse generator (figure 4) to the input of the preamplifier.

This pulse generator works as follows: The .1 μf condenser is kept charged by the battery. When the relay is switched to pin 2, the 470 pf condenser charges through 470 ohms in .2 microsecond. When the relay switches over to pin 4, the same condenser discharges through 100 K to ground in 47 microsecond. Since the relay operates on the line voltage, this yields a long pulse of 60-cycle frequency. The differentiation circuit on the output produces a short, sharp pulse (rise time .2 microsecond, fall time 50 microsecond). The opposite polarity pulses are inhibited in the preamplifier. The pulse height is accurately controlled by the 100 K helipot. Pulses of various sizes can be fed to the kicksorter, producing sharp peaks one or two channels wide. The generator is linear and can be used to calibrate the kicksorter spectra.

3. Current Integrator

The total beam striking a target was integrated over a run using the current integrator described by Edwards (1951). This device measured the voltage on a condenser which was charged by the incoming current. When the condenser reaches a certain voltage it is discharged and the cycle repeats. Two of these condensers were connected in parallel and only one was discharged, while the other continued to collect current.A schematic diagram is shown in

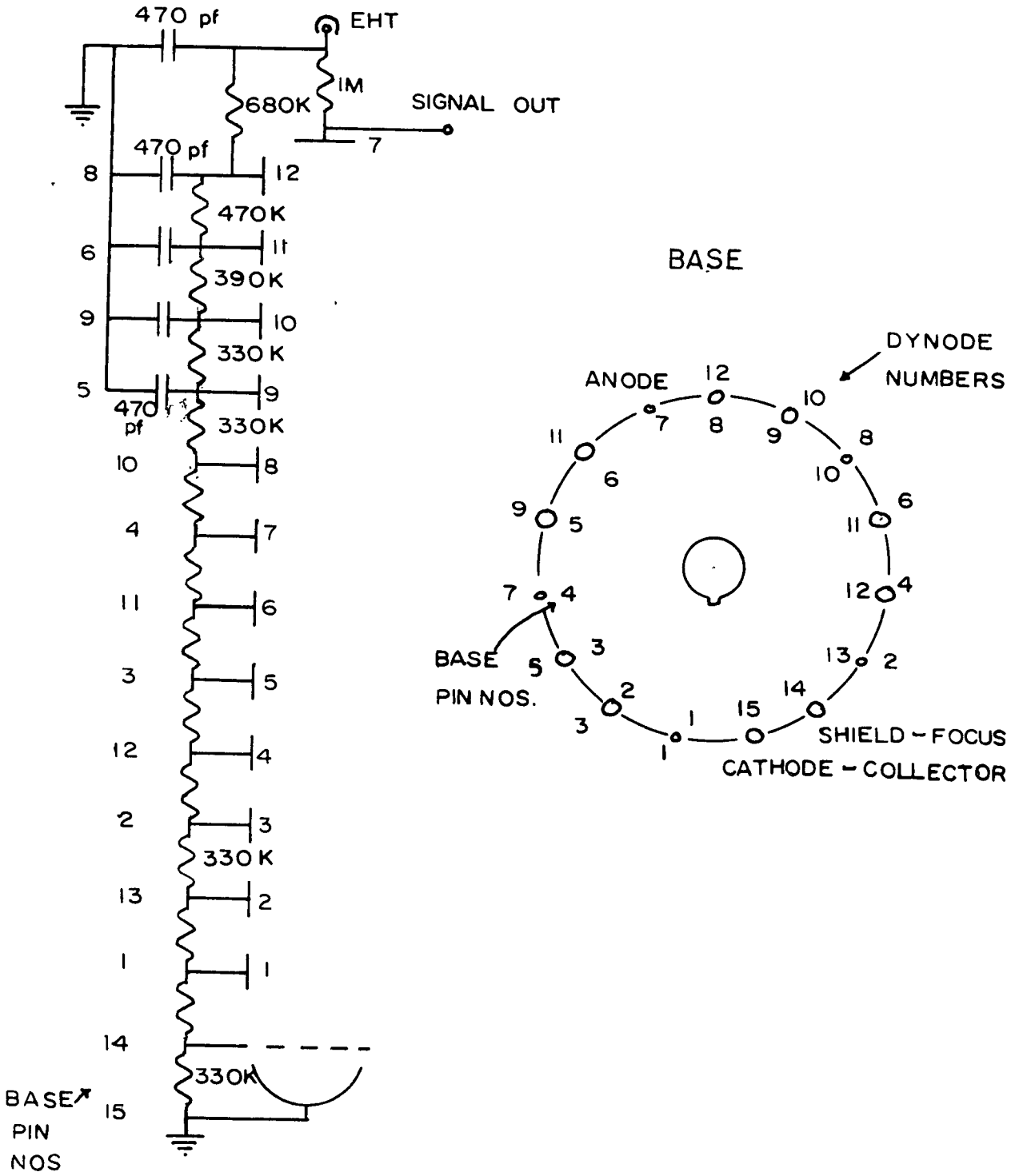

FIG. 3 PHOTOMULTIPLIER CONNECTIONS

figure 5.

Since the currents to be integrated were too large for the device to handle, they were divided into two parts, one going to ground through a 50K 1% carbofilm resistor and the other going to the instrument via a 470K 1% wire-wound resistor. The device was calibrated each day, as the voltage measurement circuit and the zero setting tended to drift.

4. Electrostatic Quadrupole Lenses

In an attempt to increase the current striking the target, a pair of electrostatic quadrupole lenses were constructed. The theory of these lenses is discussed by Enge (1959). An electrostatic quadrupole lense normally consists of four right hyperbolic cylindrical pole faces arranged in opposing pairs at right angles. To each pair is applied the same potential, one pair being charged positively and the other negatively. A charged particle entering the lens will be focused toward the axis in the plane of two of the electrodes and away from it in the perpendicular plane, since in these planes the electric field strength is proportional to the distance from the axis, to a very good approximation. Two such lenses arranged in series with corresponding poles oppositely charged produce a net focusing effect as shown by Enge.

A pair of lenses were constructed as shown in figure 6. The electrodes were made circular instead of hyperbolic, as circular sections of brass pipe were available, and mounted on rods through kovar seals.

FIG. 4 PULSE GENERATOR

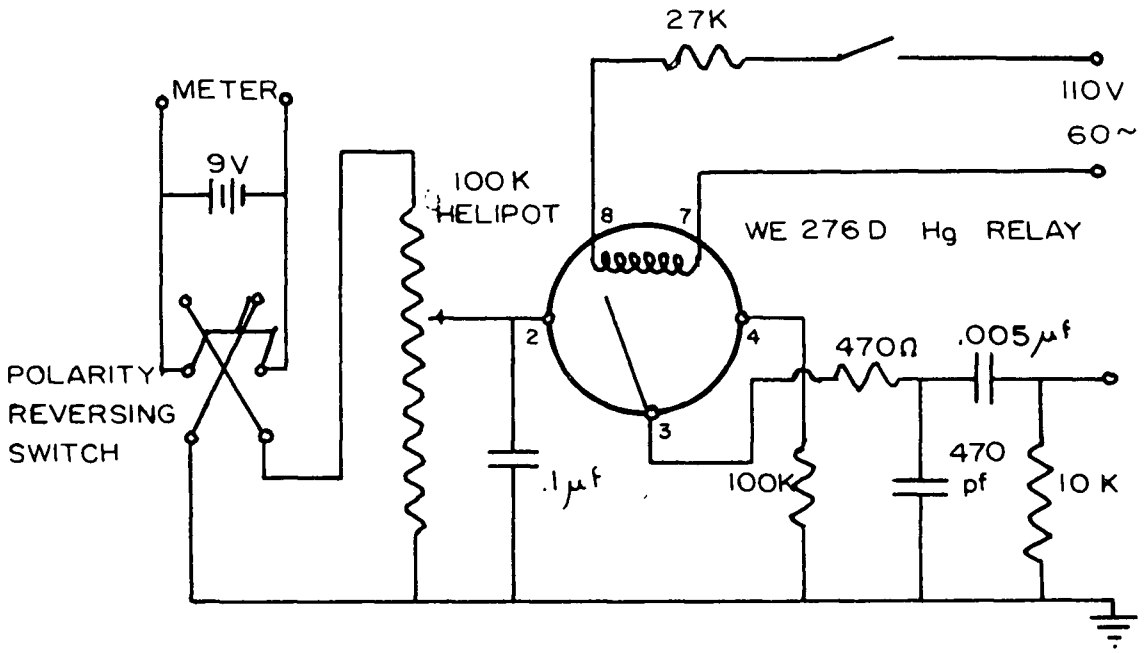

FIG. 5 CURRENT INTEGRATOR (SCHEMATIC)

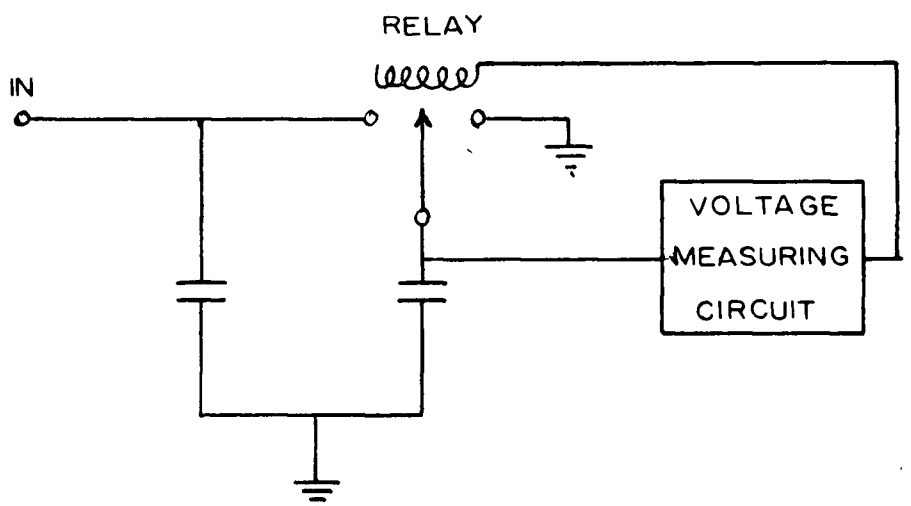

Due to the diffuseness of the beam entering the lenses, the electrodes picked up considerable current. Hence low impedance North East Instrument Company power supplies were used. Since the energy of the beam was small, the voltage required on the lenses as constructed was expected, using Enge's figures, to be less than 1000 volts even for a 45 kev beam.

The lenses were tested by placing them together after the magnet and also by placing one above and one below the magnet. When both followed the magnet, a strong focusing effect was observed. The beam could be reduced to a thin line 1/16" across either horizontally or vertically, or into an irregular spot about $\frac{1}{4}$" in diameter on the target. However, the increase in the total current was very small, indicating that even without the lenses, all the current coming through the magnet struck the target, albeit in a much larger spot than with them. A lens above the magnet had very little focusing effect at all. Hence the lenses were not used during the experimental runs.

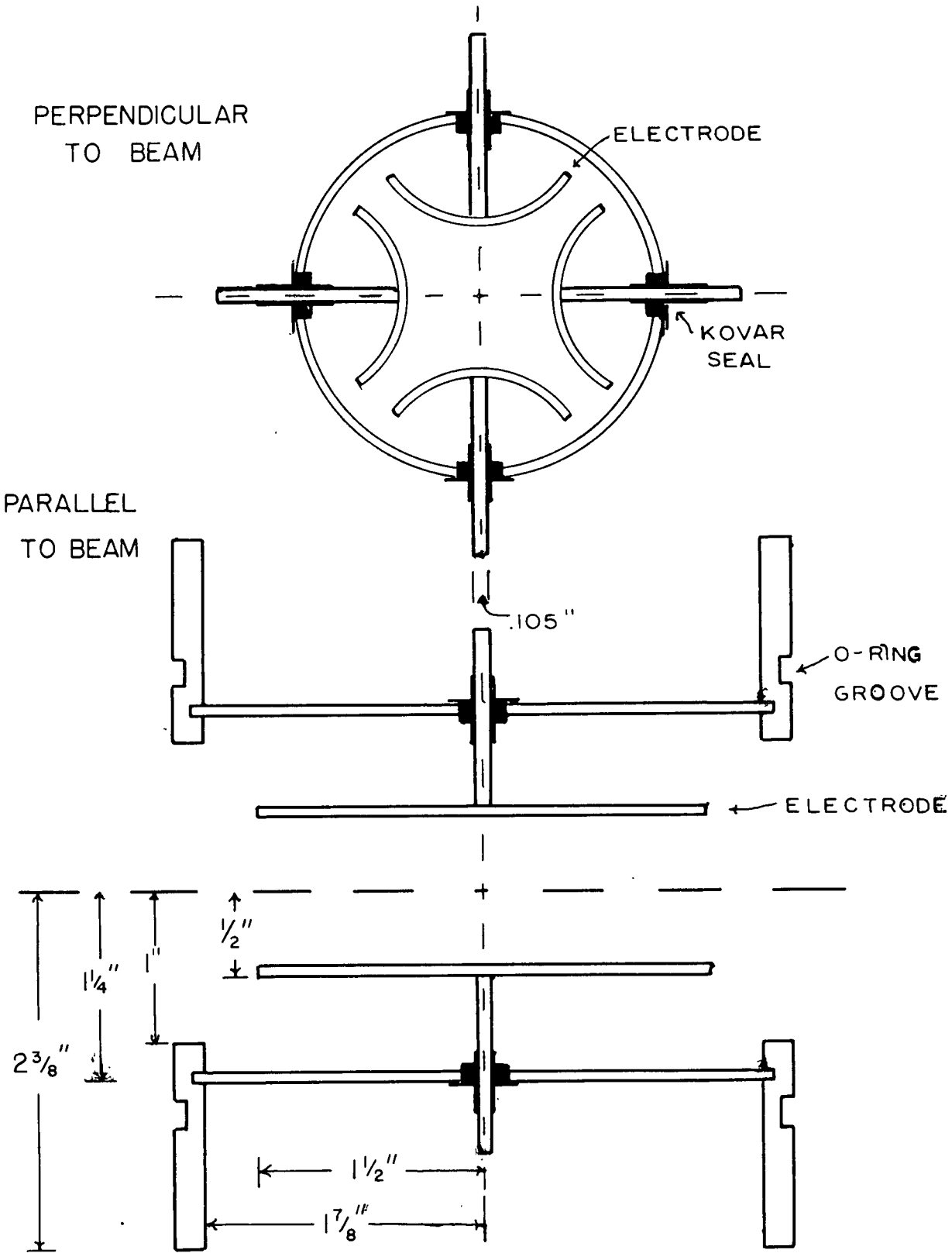

FIG. 6 QUADRUPOLE LENS – SECTIONAL VIEWS

CHAPTER III - PROCEDURE

In order to find out how many fillings of the dispenser would be necessary to produce a target thick enough to stop the beam, a rough estimate of the volume of the dispenser ($65cm^3$) was made. This, together with a knowledge of the vapor pressure of D_2O at room temperature (1.7cmHg), the density of ice and the stopping power of ice as given by Wenzel and Whaling (1952), enabled the required number of fillings to be calculated. A crude guess was made that only one fifth of the D_2O actually froze on to the target and that this froze uniformly on the backing plate. In this manner it was estimated that at 40 kev three fillings would be required. This was probably more than enough but for the purposes of this experiment it was better to have the target too thick than too thin.

After a target had been laid on the backing plate it was lowered into bombarding position and set at 30^o to the beam direction, so that no γ-rays emitted into the solid angle subtended by the counter at the 90^o position would be attenuated by passing through the copper plate. For most of the runs the counter was moved back so that its front face was 4.5cm from the target chamber, in an attempt to improve the angular resolution at the expense of the measured yield. In this manner the yield at 90^o to the beam was measured for Ep=24.0, 34.2, 40.7 and 47.2 kev. Angular distribution measurements were made at 34.2 and 40.7 kev.

The target current was measured by connecting

the top of the liquid air trap on which the target was mounted through a microammeter to the current integrator. It was found, despite the system of stops that prevented any of the direct beam from striking the walls of the target chamber, that a current equal to about 20% of the target current was picked up on the chamber. This was believed to be due to ionisation of the residual gas in the chamber by the beam. The positive ions thus produced go to the chamber walls while the elctrons are attracted to the target, causing the microammeter to read less than the actual beam current. To correct for this, the outer wall of the chamber was connected to the integrator as well as the target itself.

It was observed that the yield decreased gradually during the course of a run. This effect, known as target deterioration, was probably caused by deposition of a film of oil or other contaminant on the target. It appeared to be partly beam dependent as if the contaminant molecules were carried along by the beam. To correct for this deterioration the bombardment of each target was separated into a series of short runs over an integrated current of about thirty-five millicoulombs, and the yields extrapolated back to zero time. The yield generally decreased by half after about two hundred millicoulombs or an hour and a half of bombardment, after which period a target was discarded.

Before and after bombardment of each target the counter and electronics were calibrated by measuring the

spectrum of a 0.029 mc RdTh source superposed on one produced by the pulse generator described previously.

Several measurements of the room background were made, leaving the counter on for several hours at a time both during the day and overnight. A typical background spectrum is shown in figure 7. A total of 38 hours yielded an average value of 9.81 ± 0.07 counts per minute in the energy range 2.76 to 5.8 Mev. A measurement of the beam-dependent background made by bombarding the backing plate for 100 integrator cycles (170 millicoulombs) yielded a result of 0.0 ± 0.15 counts per millicoulomb, so that the beam dependent background was considered to be negligible. The time-dependent background was subtracted from all the runs which were also corrected for absorption in the target chamber and for counter efficiency. The efficiency, as defined, has been shown to be independent of source distance, so no additional correction was necessary for the short range used.

Since the velocity of the He^{3*} nuclei formed was expected to be small, the Doppler shift correction discussed by Griffiths and Warren (1955) was neglected.

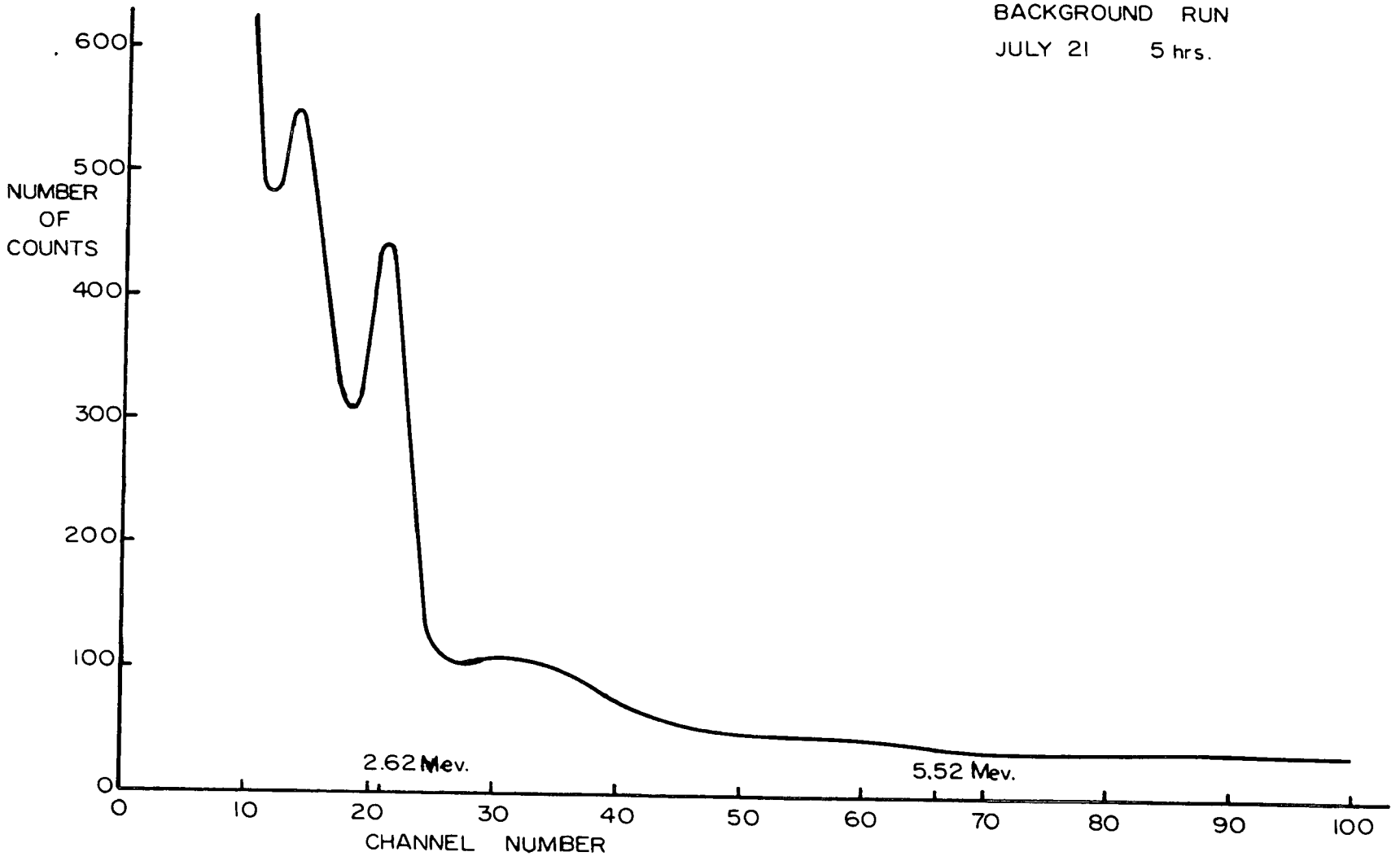

FIG. 7 A TYPICAL BACKGROUND SPECTRUM

CHAPTER IV - RESULTS

1. Angular Distribution

As the angular distribution was expected to conform to the $(\sin^2\theta + B)$ relation found at higher energies by Fowler et al., the chief interest in measuring it lay in the determination of the size of the isotropic component. In any case, due to the low yield and resulting poor statistics, it was expected that an attempt to detect deviation from this relation would lead to inconclusive results. Therefore, a simple estimate of the value of B was obtained by measuring the yields at 90° and zero degrees. To permit correction for target deterioration the counter was moved back and forth from 90° to 0° several times during the bombardment on each target. One measurement at 45° gave a result in accord with the $\sin^2\theta$ distribution, to within the statistical error. Angular distribution measurements were made at 34.2 and 40.7 kev but not at 24.0 and 47.2 kev, since at 24.0 the yield was very low, and at 47.2 the apparatus became unstable, tending to produce high tension sparks or discharges from the oscillator coil, which sent large surges back into the supply lines, blowing fuses, cutting off the ion source discharge, and sometimes even stopping the kicksorter. Spectra at 90° and 0° are shown in figure 8.

Since the counter subtended a finite solid angle at the target, the measured angular distribution was somewhat smeared. That is, the measured number of

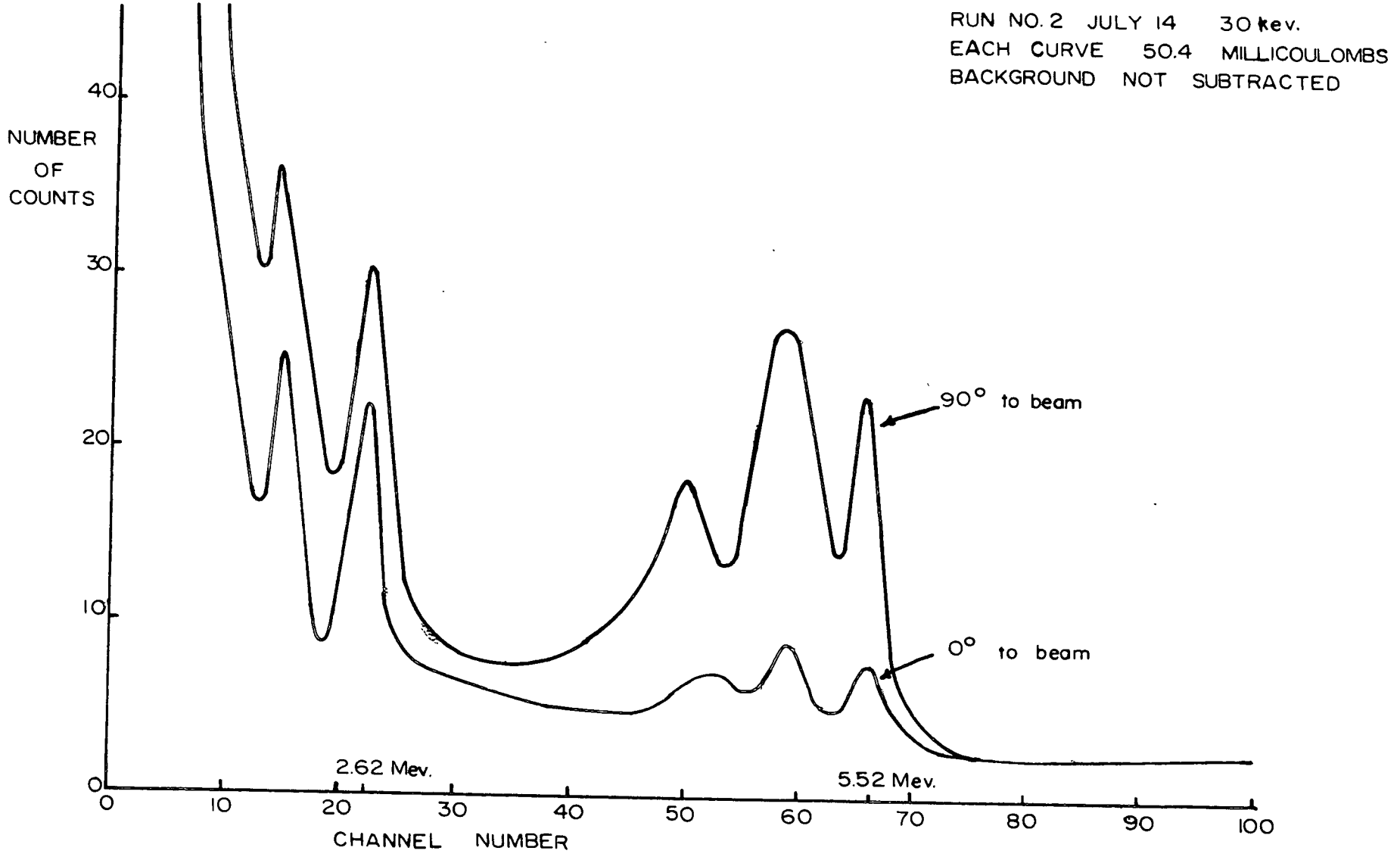

FIG. 8 TYPICAL $D(p,\gamma)He^3$ SPECTRA

counts at 90° was somewhat less than the differential yield exactly at 90°, and the number at 0° correspondingly too high, leading to a high estimate of B. This was corrected by using a modification of a method devised by Rose (1953) for correcting angular correlation data for the same effect.

If the distribution is of the form

$$(1)\quad W(\theta) = \sum_n a_n P_n(\cos\theta)$$

and is measured by a cylindrical crystal of length t and radius r, distant h from the source, the measured distribution will be

$$(2)\quad \bar{W}(\theta) = \frac{\int W(\theta')(1-e^{-\tau x})d\Omega}{\int (1-e^{-\tau x})d\Omega}$$

where Ω is the crystal solid angle, τ is its absorption coefficient (Grodstein 1957) and x is the distance travelled through it by the γ-ray. If β is the angle between the ray and the crystal axis, x is given by

$$x(\beta) = t\sec\beta \qquad 0 \le \beta \le \tan^{-1}\frac{r}{h+t} = \beta'$$

$$x(\beta) = r\csc\beta - h\sec\beta \qquad \beta' \le \beta \le \tan^{-1}\frac{r}{h} = \gamma'$$

Furthermore, since $\theta' = \theta + \beta$, $P_1(\cos\theta') = P_1(\cos\theta)P_1(\cos\beta) +$ azimuthal terms which do not contribute to the integral. By substituting (1) into (2) it is easy to see that $\bar{a}_n$ the coefficient of P_n in $\bar{W}(\theta)$ should be corrected by

a factor J_o/J_n where

$$(3)\quad J_n = \int_0^{\gamma} P_n(\cos\beta)(1-e^{-\tau x(\beta)})\sin\beta\, d\beta .$$

Only two terms of the series, P_o and P_2, are required to fit a $\sin^2\theta$ distribution since

$$A(\sin^2\theta + B) = 1 + aP_2(\cos\theta) = 1 + \frac{a}{2}(3\cos^2\theta - 1)$$

yields

$$a = -\frac{1}{\frac{3B+1}{2}} \quad \text{or} \quad B = -\frac{2(1+a)}{3a}$$

Therefore if $a = \frac{J_o}{J_2}\,\bar{a}$,

$$B = -\frac{2}{3} - \frac{2}{3a} = -\frac{2}{3} + \frac{2J_2}{J_o 3}\left(\frac{3\bar{B}}{2} + 1\right)$$

$$(4)\quad = -\frac{2}{3} + \frac{2J_2}{3J_o} + \bar{B}\,\frac{J_2}{J_o}$$

Values of J_o and J_2 were found by graphical integration for the values of h used in this experiment. For the value at which the angular distributions were measured, 8.1 cm from the center of the target to the front face of the crystal, the value of J_2/J_o is 0.914.

The measurements at 0^o had also to be corrected for absorption in the backing plate which was found to be 0.0319 $\pm$0.007 or 0.0811$\pm$0.0018 cm thick. The absorption coefficients for this and for the brass of the target chamber were taken from Davisson and Evans (1952).

The values of B obtained were

E_p(kev)	B
34.2	0.27$\pm$0.11
40.7	0.295$\pm$0.11

The errors quoted are statistical in nature.

Thus the percentage of isotropic contribution is considerably larger at these energies than it was in the 300 kev to 1 Mev range. The evidence is inconclusive as to whether or not it is still increasing as the energy decreases.

2. The Absolute Cross Section

The absolute cross section for a reaction is defined as the integral of the differential cross section over all angles. Hence to obtain the absolute cross section it is first necessary to know the total thick-target yield per incident proton, integrated over all angles. Since the angular distribution is approximately known, the total yield can be obtained directly from the differential yield at 90° by integration.

For this purpose, at each energy, a series of runs was taken on a single target and the number of counts per millicoulomb, with background subtracted, was plotted against time and extrapolated back to the start of bombardment (see figure 9). The angular distribution runs were plotted similarly and served as an initial check on the deterioration. The initial yield figures for each energy were averaged and corrected for counter efficiency (multiplication factor $\frac{1}{.73} = 1.37$) and for absorption in the 1/16" brass of the target chamber (factor 1.04) using an average (weighted 67 Cu33 Zn) of the absorption coefficients given by Davisson and Evans (1952) for copper and zinc.

The error introduced by the finite solid angle subtended by the counter at the target was corrected by the following method. Let $N=A(\sin^2\theta + B)$ be the number

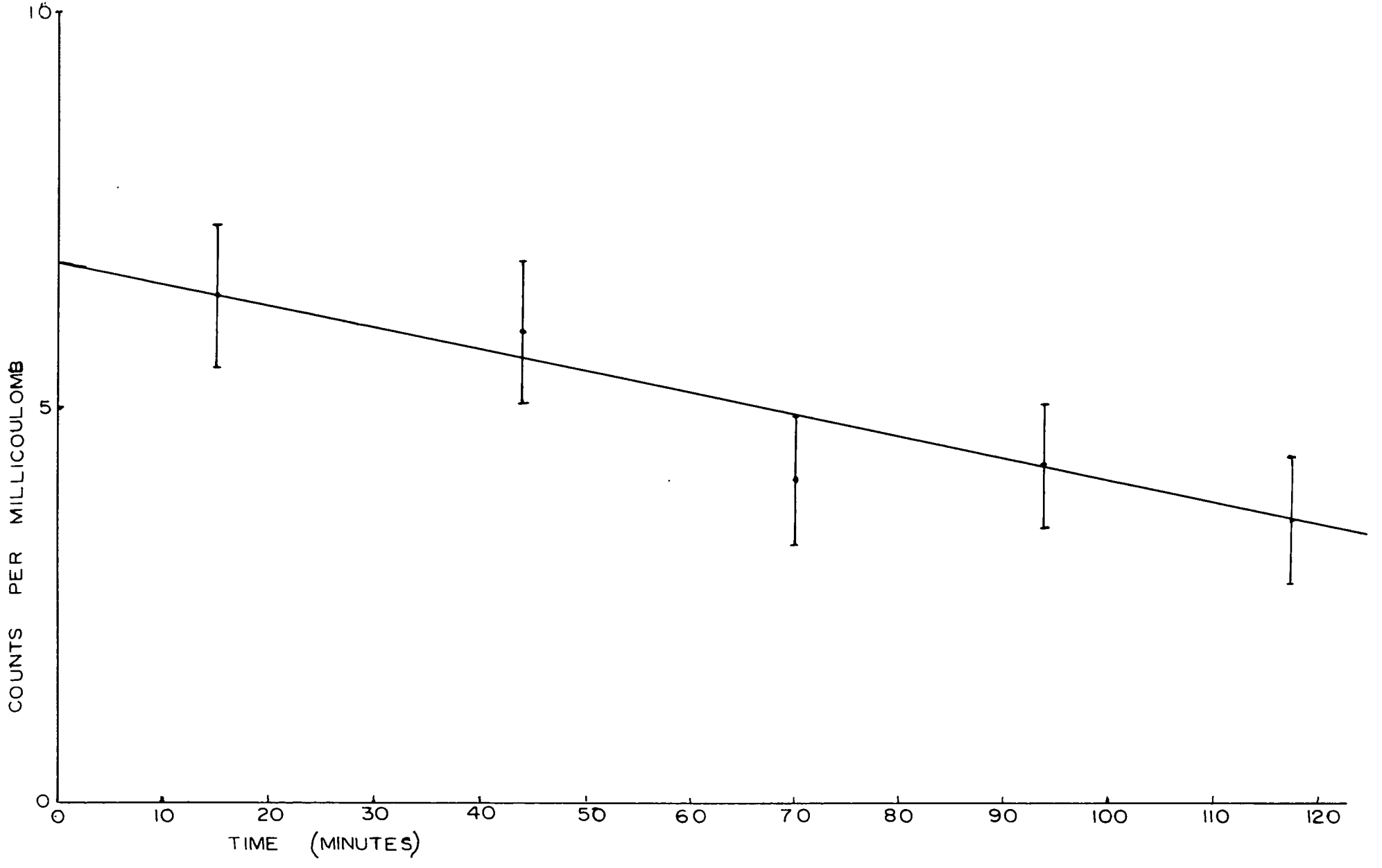

FIG. 9 DETERIORATION OF A TARGET

of γ-rays per unit solid angle. If x is the number emitted at 90° into the counter solid angle, ω_o , then a value of A may be obtained from x using $x=A_e(1+B)\omega_o$. This value is incorrect, however, as it assumes uniform intensity over the entire area of the counter. Correctly, A may be obtained from

$$x = A_c\int_{\omega_o} (\sin^2\theta + B)\frac{dS}{r^2} = A_c I_c$$

where dS is the unit of surface area on the plane parallel to the counter face through its effective center. By changing variables from r, θ , and ϕ , the angle of rotation about the beam direction, to D the distance from the target to the effective center of the crystal, x the distance in the effective center plane away from the center, and β the angle in this plane we obtain:

$$\omega_o = \int_o^R \int_o^{2\pi} \frac{x\,dx\,d\beta}{D^2+x^2} = \pi \log\left(1+\frac{R^2}{D^2}\right)$$

and

$$I_c = \int_o^R \int_o^{2\pi} \frac{D^2\,x\,dx\,d\beta}{(D^2+x^2)(D^2+x^2\cos^2\beta)} + B\,\omega_o$$

where R is the crystal radius. I_c can be integrated by partial fractions and expansion of $\log(1+Z)$ to obtain a solution in series form. Substitution for all the terms greater than .1% of the largest term yields the following results.

D(cm)	ω_o (steradians)	I_c	$\frac{A_c}{A_e} = \frac{\omega_o (B+1)}{I_c} = C$
7.7	.592	.732	1.037±.003
8.9	.451	.563	1.028±.003
11.8	.265	.334	1.018±.002
12.4	.241	.304	1.016±.0015

The last column is included to indicate the size of the error incurred by assuming that the intensity is constant over the counter solid angle. In this calculation B was assumed to take on the value 0.283, the average of the two values previously obtained. This assumption that B is constant throughout the narrow energy range of this experiment should not lead to serious errors. Values of A at each energy were calculated using $A = \frac{Cx}{(1+B)\ \omega_o}$

Now the total yield is given by

$$Y = A \int_o^{2\pi} \int_o^{\pi} (\sin^2\theta + B)\sin\theta \ d\theta \ d\phi$$

$$= \frac{4}{3}\pi A(2+3B)$$

Values of Y were calculated using

$$(6)\quad Y = \frac{4\pi Cx(2+3B)}{3(1+B)\ \omega_o}\ 1.6 \times 10^{-16}\ \gamma\text{-rays/proton.}$$

These are tabulated below

kv	A(γ-rays per unit solid angle per millicoulomb)	Y(γ-rays per incident proton x 10^{-14})
24.0	17.4±3.3	3.34±0.45
34.0	41.0±5.8	7.82±0.65
40.7	75.9±10.9	14.5±1.3
47.2	114.3±14.6	21.8±1.6

The total thick target yield Y is plotted against incident proton energy in figure 10.

To obtain the cross-section as a function of energy from the thick target yield, the theory of a thick target must be considered. A thick target is defined as one in which all the bombarding particles come to rest. At any distance x into the target where the bombarding particles are still moving with energy E,

$$dY = 2N dx\ \sigma(E) = 2N \frac{dx}{dE}\sigma(E)dE$$

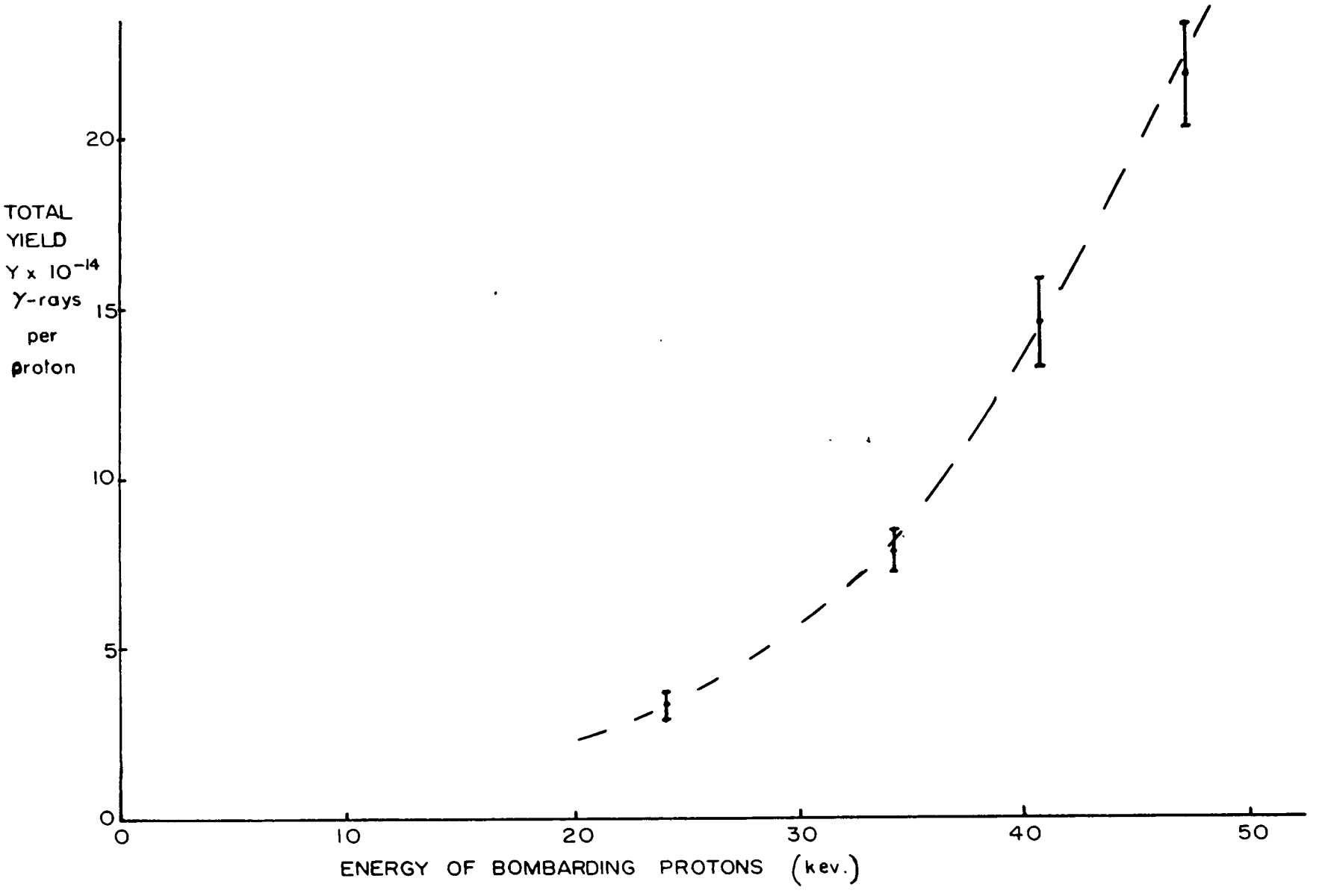

FIG. 10 TOTAL YIELD CURVE

where N is the number of D_2O molecules per cubic centimeter of target and $\sigma(E)$ is the cross-section in square centimeters. The factor 2 appears because there are two deuterium atoms in each D_2O molecule.

The stopping power $\frac{dE}{dx}$ is defined in terms of the molecular stopping cross-section ϵ by $\frac{dE}{dx} = -N\ \epsilon(E)$ Using this stopping cross-section, the yield is given by

$$(7)\quad Y(E_1) = \int_0^{E_1} \frac{2\ \sigma(E)}{\epsilon(E)}\ dE$$

There have been several attempts made to determine $\epsilon(E)$ for protons in water. Hirschfelder and Magee (1948) calculated, using a theory due to Bethe, the values of the stopping number B for hydrogen and oxygen, where

$$\epsilon = 2\ \pi\ e^4\ \frac{M}{m}\ \frac{B(E)}{E}$$

In this equation e is the electronic charge and M/m is the ratio of the mass of the proton to that of the electron. A simple addition (Bragg theory) of the stopping cross-sections thus obtained gives a value of ϵ for H_2O in excellent agreement with the experimental results of Wenzel and Whaling (1952) for D_2O ice. In this latter work, it was assumed that the cross-section for $O^{16}(p,p)O^{16}$ scattering was given by Rutherford's formula and ϵ calculated from the yield of scattered protons from D_2O ice. However, later work by Phillips (1953) and Reynolds et al. (1953) on hydrogen, oxygen and water vapor suggests that the stopping cross-section for water vapor is 15-20% higher than Hirschfelder and Magee estimated and, furthermore, that it is not equal to a simple sum of those for hydrogen and

oxygen. The various estimates are plotted in figure 11 with the errors quoted for them. Since Wenzel and Whaling's values for D_2O ice were for conditions closest to those employed in this work, they have been used in the following calculations.

There are several ways to calculate σ from equation (7). One is simply to differentiate Y so that

$$\left.\frac{dY}{dE}\right|_{E_1} = \frac{2\ \sigma(E_1)}{\epsilon(E_1)}$$

This gives σ at once. However, the slope of the yield curve is not clearly determined, especially at the end points 24.0 and 47.2 kev. The errors thus incurred are rather large and indeterminate, so this method was abandoned.

An estimate of the slope of the yield curve with a better known error can be obtained by taking the difference between the measured points and by assuming that the $\Delta Y/\Delta E$ thus obtained is the slope at the mid-point of the interval. Since the curve is smooth and nearly a straight line, especially at the upper energies, this should give a good estimate of the energy at which $\Delta Y/\Delta E$ is supposed to take on the value obtained. Then $\Delta Y/\Delta E$ can be equated to $2\sigma/\epsilon$ at the midpoint. This, of course, cuts by one the number of cross-section points obtained, but it is expected that the statistical errors quoted are accurate estimates. These results are plotted as Method 1 in figure 12.

If the cross-section is assumed to be controlled by penetrability considerations, as it is expected to be

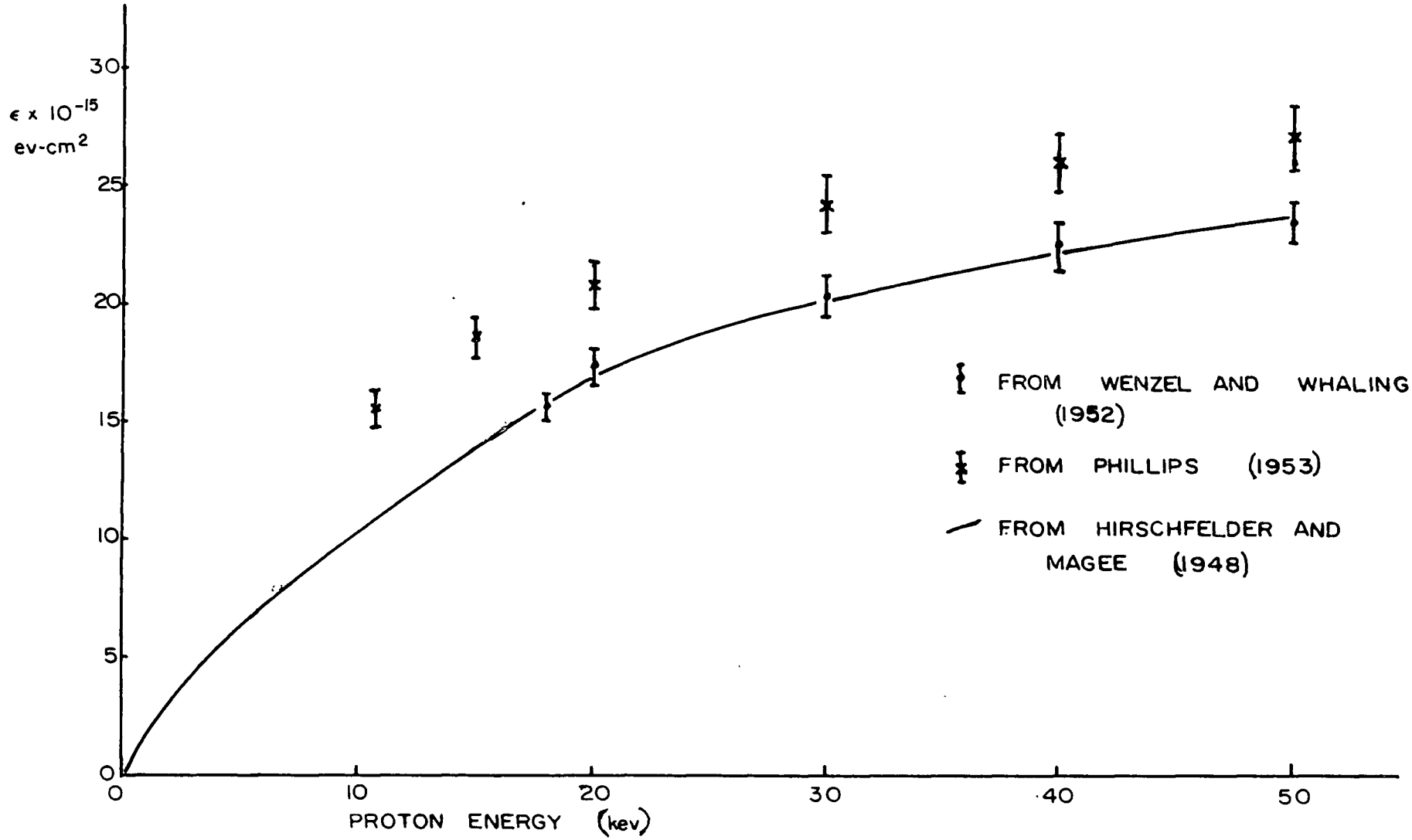

FIG. 11 STOPPING CROSS-SECTION FOR PROTONS IN D_2O

at the energies involved in this experiment, it should have an energy dependence of the form

$$\sigma = KE^{-1}\exp - \left(\frac{\sqrt{2}\,\pi\, e^{2} M^{\frac{1}{2}}}{h} E^{-\frac{1}{2}}\right)$$

where M is the proton mass and K is a constant. Values of σ/K can be calculated and $\frac{2\sigma}{K\epsilon}$ plotted as a function of energy. This can be integrated using a planimeter and a value of $\frac{Y}{K}$ obtained for any desired energy. Using the experimental values of Y, values of K can be obtained. The results are given below:

E(kv)	$Y/K \times 10^{12}(\text{kev cm}^2)^{-1}$	$Y \times 10^{-14}$	$K \times 10^{-28}$ kev cm^2
24.0	57.5±2.3	3.34±0.45	5.81±1.02
34.2	161.3±6.5	7.82±0.65	4.84±0.58
40.7	256.3±10.3	14.7±1.3	5.65±0.73
47.2	370.0±14.8	21.8±1.6	5.89±0.67
		Average	5.52±0.77

Using these values of K and the calculated values of σ/K, the following values of σ were obtained and plotted in figure 9 as Method 2.

E(kv)	$\sigma/K(\text{kev}^{-1})$	$\sigma \times 10^{-32}$ cm^2
24.0	6.91×10^{-5}	4.09±0.71
34.2	1.47×10^{-4}	6.63±0.81
40.7	1.79×10^{-4}	10.11±1.31
47.2	2.22×10^{-4}	13.04±1.48

As can be seen these give a reasonable agreement with Method 1.. A plot of the function

$$\sigma = 5.52\times10^{-28}E^{-1}\exp -\left(1.254\times10^{-3}E^{-\frac{1}{2}}\right)$$

is included in figure 9.

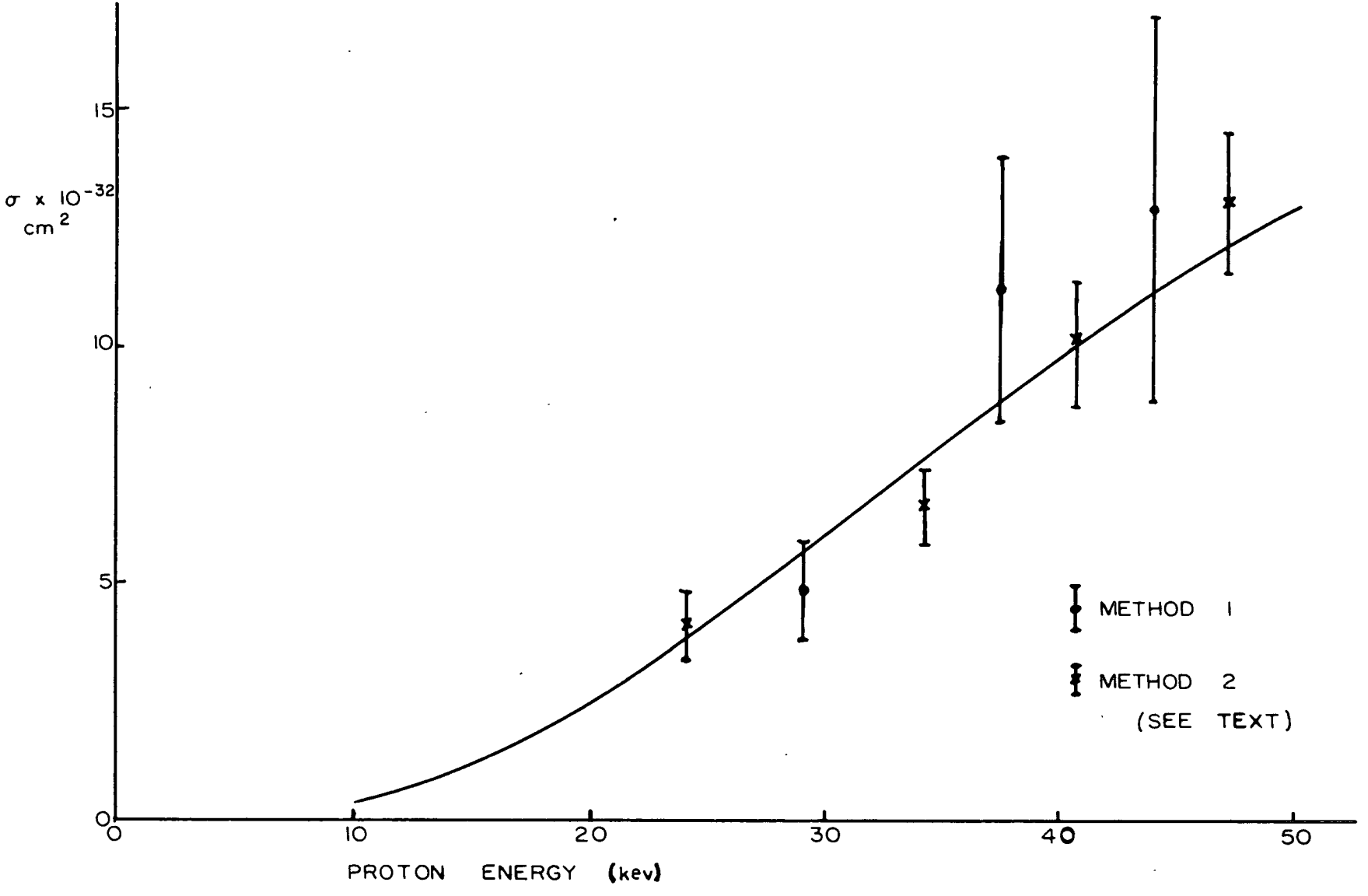

FIG. 12 TOTAL CROSS-SECTION FOR $D(p,\gamma)He^3$

CHAPTER V - CONCLUSIONS

The errors quoted in the above results and indicated in the graphs are purely statistical in nature. Some other errors have been discussed and corrected. However, there are some uncertainties incurred in this experiment which should be discussed.

The effective center depth and efficiency of the counter were measured for a broad parallel flux of γ-rays. In our experiment, due to the close proximity of the counter to the target, this was not the case because the γ-rays emanated from a small source. Hence a few γ-rays might be detected in a larger solid angle than that quoted. Since they passed through a relatively small thickness of crystal, however, they were less likely to be detected. Hence the error incurred here is likely to be not bigger than the solid angle corrections involved in the angular distribution function calculation, say about 5%.

There is a small uncertainty (2mm) in the positioning of the spot on the target where the beam struck, leading to an error of about 2% in D the distance to the effective center. This added to the 0.5 cm uncertainty in the position of the effective center makes an error of about 10%.

Runs were made at three different distances (and corrected for target deterioration)to check the position of the effective center for the small counter-to-

target distances used in this work. The results are plotted in figure 13. The effective center deduced from these results agrees, to within the statistical error, with the 5.5cm±0.5cm effective center depth found for the counter previously.

It has been mentioned that there was a considerable current detected on the walls of the target chamber despite the fact that the beam was collimated so that it fell entirely on the target. This current was believed to be due to ionisation of the residual gas in the chamber, and to correct for it the chamber was connected to the target. However, some of the ions thus formed may have been repelled by the +150V on the target chamber and collected elsewhere. Furthermore, the chamber may have collected a small number of secondary electrons from other parts of the tube, increasing the difference between the actual beam intensity and that calculated from the measured current. The magnitude of this uncertainty is estimated to be not more than 5%.

Due to the lack of energy-defining slits in the magnet system, the precise kinetic energy of the protons incident on the target is unknown. Errors due to the size of the beam above the magnet and the magnet dispersion, together with uncertainties in the calibration of the 60 megohm resistor chain, fluctuations in the high tension supplies and the Maxwellian velocity distribution in the ion source, lead to a further 5% uncertainty in the energy of the bombarding protons.

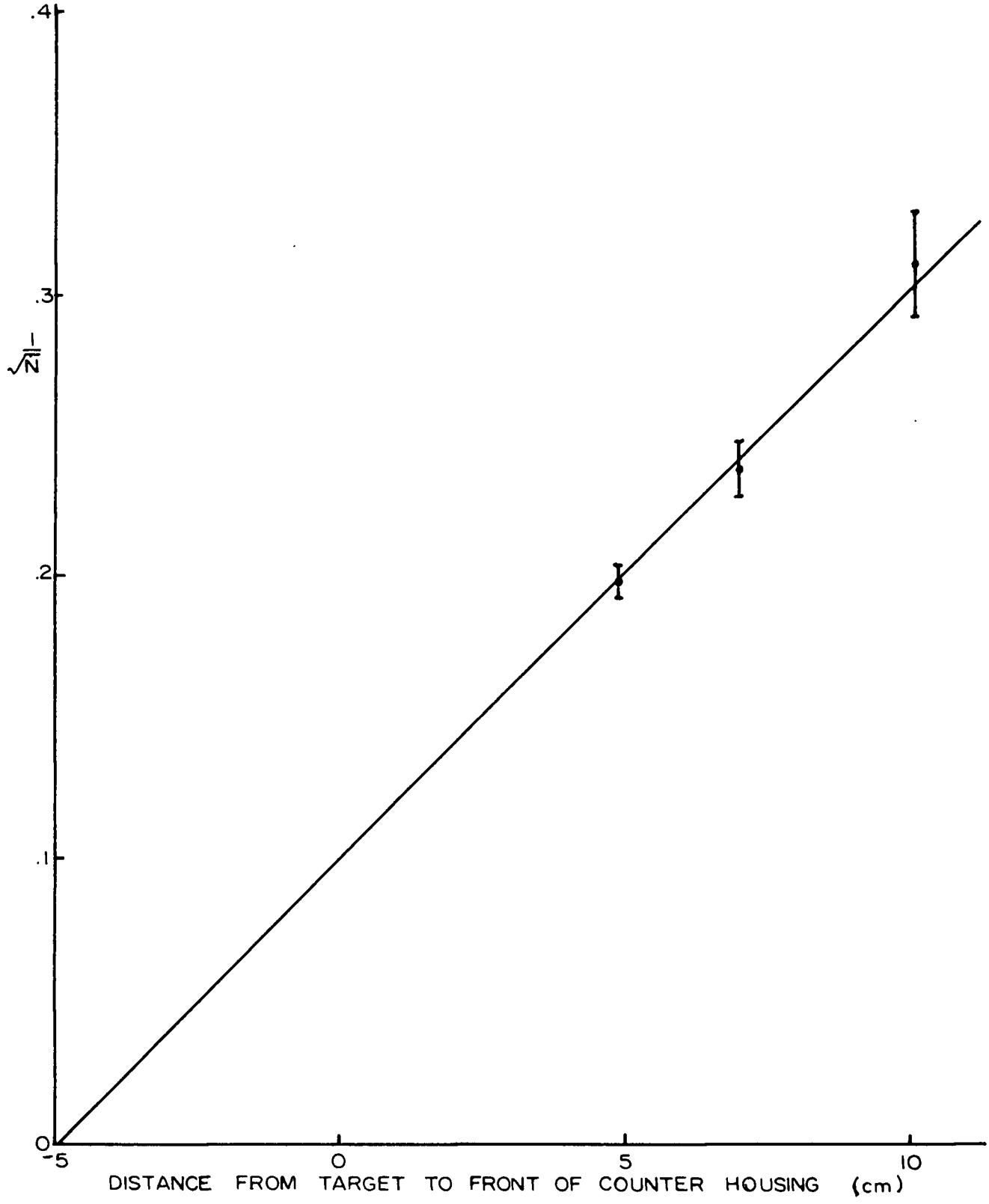

FIG. 13 VARIATION OF COUNTING RATE WITH DISTANCE

N = COUNTS PER MILLICOULOMB

Thus the following errors have not been accounted for in our estimate of the cross-section.

Point source effect	5%
Source to counter distance	10%
Unmeasured current	5%
Dispersion	5%
Total estimated error	14%

The error in the angular position of the counter was about 2%, too small to increase this total. Other small uncertainties such as drift in electronics, and fluctuations in the magnet current are expected to contribute no more than 1% to the error.

Hence we may conclude from this experiment that at low bombarding energies the cross-section for $D(p,\gamma)He^3$ increases rapidly with energy, as is expected if it depends chiefly on exponential penetrability. The s-wave component of the gamma ray yield is much larger relative to the p-wave contribution than it was found to be at higher energies, indicating a different energy dependence for each component. A more detailed study would be required to separate the two components as functions of energy.

It seems likely from the fact that the "isotropic" component decreases less rapidly with energy, that it actually is an s-wave contribution and hence is really isotropic and that its true angular dependence is not obscured by the p-wave dependence. However, a much more accurate measurement of the angular distribution, taken more slowly to permit larger yields and at many more angles would be re-

quired to prove this. Suffice it to say, however, that this work yields results in fair agreement with theoretical predictions and serves as a basis for further investigations, both experimental and theoretical in nature.

BIBLIOGRAPHY

1. Cameron, A.G.W., Private Communication, with Dr. G.M. Griffiths, 1960

2. Curran, S.C. and Strothers, J., Proc. Roy. Soc. 172, 72, 1939

3. Davisson, C.M., and Evans, R.D. Rev. Mod. Phys. 24, 79, 1952

4. Edwards, M.H., M.A. Thesis, U.B.C. 1951

5. Enge, H.A., Rev. Sci. Inst., 30, 248, 1959

6. Fowler, W.A., Lauritsen, C.C., and Tollestrup, A.V., Phys. Review. 76, 1767, 1949

7. Griffiths, G.M. and Warren, J.B., Proc. Phys. Soc. 68, 781, 1955

8. Grodstein, G.W., N.B.S. Report 583, 1957

9. Kirkaldy, J.S., M.A. Sc. Thesis, U.B.C. 1951

10. Lal, M., Ph.D. Thesis, U.B.C. 1961

11. Larson, E.A.G., M.A. Thesis, U.B.C. 1957

12. Phillips, J.A., Phys. Rev. 90, 532, 1953

13. Reynolds, H.K., Dunbar, D.N.F., Wenzel, W.A., and Whaling, W., Phys. Rev. 92, 742, 1953

14. Rose, M.E., Phys. Rev., 91, 610, 1953

15. Singh, P.P., Griffiths, G.M., Ssu, Y.I., and Warren, J.B. Can. J. Phys., 37, 866, 1959

16. Wenzel, W.A., and Whaling W., Phys. Rev., 87, 610, 1952

17. Wilkinson, D.H., Phil. Mag. 43, 659, 1952